

## Supporting information

### **Bone-Targeted Calcification–Photothermal Nanoplatfom for Synergistic Tumor Ablation and Bone Regeneration in Breast Cancer Bone Metastasis**

*Zhili Ran, Xinyi Li, Guibo Lu, Jiapeng Dong, Yaoxun Zeng, Junze Tang, Huiling Ye, Guining Cao, Yikun Shang, Ziyue Li, Qionge Sun, Xiang Su, Yan He\*, Xujiu Liu\**

Z. Ran, X. Li, G. Lu, J. Dong, Y. Zeng, H. Ye, G. Cao, X. Su, Y. He, X. Liu

School of Biomedical and Pharmaceutical Sciences

Guangdong University of Technology

Guangzhou 510060, China.

E-mail: [heyuan129@gdut.edu.cn](mailto:heyuan129@gdut.edu.cn); [liuxujiu@gdut.edu.cn](mailto:liuxujiu@gdut.edu.cn)

J. Tang, Y. Shang, Z. Li, Q. Sun

College of Traditional Chinese Medicine

Yunnan University of Chinese Medicine

Kunming 650500, China.

## Experimental Section

### Materials

Calcium chloride ( $\text{CaCl}_2$ ), Sodium chloride ( $\text{NaCl}$ ), Ascorbic acid (AA), Glycero 2-phosphate disodium salt ( $\text{C}_3\text{H}_7\text{Na}_2\text{O}_6\text{P}\cdot 5\text{H}_2\text{O}$ ), and Dexamethasone (DXMS) were purchased from Sigma-Aldrich Corporation Co., Ltd. (Shanghai, China). Polyvinyl pyrrolidone (PVP, MW58000), Dimethyl sulfoxide (DMSO), 1-Hexadecylpyridin-1-ium chloride ( $\text{C}_{21}\text{H}_{38}\text{ClN}$ ), Calcein ( $\text{C}_{30}\text{H}_{26}\text{N}_2\text{O}_{13}$ ), Hydrogen peroxide solution ( $\text{H}_2\text{O}_2$ ), Fluorescein isothiocyanate (FITC), and 3-(4,5-dimethyl-2-thiazolyl)-2,5-diphenyl-2-H-tetrazolium bromide (MTT) were purchased from Aladdin Biochemical Technology Co., Ltd. (Shanghai, China). MTT was purchased from Huayun biotech Co., Ltd. (Guangzhou, China). Dopamine hydrochloride (DOPA), phytic acid dodecasodium (PA-Na), and Palladium chloride ( $\text{PdCl}_2$ ) were purchased from Macklin Biochemical Co., Ltd. (Shanghai, China).  $\text{PdCl}_2$  was purchased from Senrise Technologies Co., Ltd. (Anhui, China). Ammonium hydroxide ( $\text{H}_5\text{NO}$ ), Ethanol absolute ( $\text{C}_2\text{H}_5\text{OH}$ ) were purchased from Damo chemicals reagent factory (Tianjin, China). Fetal bovine serum (FBS) was purchased from ExCell (Cat# FSP500, Shanghai, China). 0.25% trypsin-EDTA, Penicillin streptomycin,  $\alpha$ -MEM basal medium, and Roswell park memorial institute (RPMI) 1640 medium were obtained from Procell Life Science&Technology Co.,Ltd. (Wuhan, China). Phosphate-buffered saline (PBS), 4% Paraformaldehyde, and Calcium content assay kit were purchased from Biosharp (Beijing, China). Hoechst33342 staining solution, Fluo-4 AM, Alizarin red S staining solution, Calcein acetoxymethyl ester (Calcein AM), Propidium iodide (PI), and Annexin V-FITC/PI apoptosis detection kit were purchased from Solarbio Science&Technology Co.,Ltd. (Beijing, China). 1,1'-Diocadecyl-3,3',3'-tetramethylindodicarbocyanine,4-chlorobenzenesulfonate salt (DiD), Mito-tracker deep red 633, ALP assay kit, Enhanced BCA protein assay kit, Cell mitochondria isolation kit (JC-1), 2,7-Dichlorofluorescein diacetate (DCFH-DA), LDH assay kit, Reactive oxygen species assay kit, and  $\text{H}_2\text{O}_2$  assay kit were purchased from Beyotime Institute of Biotechnology (Jiangsu, China). Monoclonal antibodies against HSP70 were purchased from Abcam (Cambridge, UK). Gelnest matrix, Cell culture dishes/plales, Cell chambers, 20 mm glass-bolloon dishes, and centrifuge tubes were obtained from NEST Biotechnology (wuxi, China). All aqueous solutions were prepared using ultrapure water (resistivity  $18.2\text{ M}\Omega\cdot\text{cm}$ ). All other chemicals and reagents were of analytical grade and used as received from Aladdin Biochemical Technology Co., Ltd. (Shanghai, China) without further purification.

## Characterization

Nanoparticle dispersions were dropped onto 300-mesh carbon-supported copper grids and imaged using a HT 7700 field-emission transmission electron microscope (TEM) (Hi-BON, Japan) to examine their morphological features. The morphology and elemental composition of nanoparticles were further characterized by a Talos F200S field-emission TEM (FEI, USA), equipped with an energy-dispersive X-ray spectroscopy (EDS) system for elemental analysis and mapping. The morphology and elemental distribution of calcified cells were examined using a LYRA 3 XMU focused ion beam field-emission scanning electron microscope (SEM) (TESCAN, Czech Republic) coupled with an EDS detector for elemental mapping. The hydrodynamic diameter, polydispersity index (PDI), and zeta potential of the nanoparticles were measured using a zeta potential and particle size analyzer (BIC, USA). Ultraviolet–visible–near-infrared (UV–vis–NIR) absorption spectra were obtained using a UV-3600 Plus spectrophotometer (PerkinElmer, USA). Fourier-transform infrared (FTIR) spectra were collected using an iS50R full-spectrum infrared workstation (Thermo Fisher Scientific, USA). The chemical valence states of the elements in the samples were analyzed *via* X-ray photoelectron spectroscopy (XPS) using a K-Alpha spectrometer (Thermo Scientific, USA). X-ray diffraction (XRD) patterns were acquired with an Ultima III diffractometer equipped with a Cu K $\alpha$  radiation source (Rigaku, Japan). The optical absorbance of nanoparticle suspensions was measured using a multifunctional microplate reader (Paradigm, USA). First and second near-infrared (NIR-I and NIR-II) laser irradiations were generated by continuous-wave diode lasers at 808 nm and 1064 nm, respectively (Xi'an Leize Electronic Technology Co., Ltd., China). Real-time temperature monitoring and thermal imaging were conducted using a 326Pro infrared thermal imaging system (FOTRIC, China). Cellular imaging was performed using a laser scanning confocal microscope (ZEISS LSM 800 with Airyscan, Germany). Flow cytometry (Merck, USA) was employed for cell apoptosis analysis. *In vivo* imaging of mouse tibiae was carried out using a U-OI/CT multimodal optical and X-ray computed tomography system for small animals (Milabs B.V., Netherlands).

## Preparation of CaO<sub>2</sub> nanoparticles

Polyvinylpyrrolidone (PVP, 0.3 g) was dissolved in absolute ethanol (15 mL) *via* ultrasonication. Subsequently, 1 mL of calcium chloride solution (0.1 mg mL<sup>-1</sup>) was added dropwise under continuous stirring at room temperature for 30 minutes. Then, 30% hydrogen peroxide (200  $\mu$ L) and aqueous ammonia (300  $\mu$ L) were added sequentially. The reaction mixture was stirred for 2 hours. The resulting

product was collected by centrifugation at 12000 rpm for 20 minutes, washed three times with absolute ethanol, filtered through a 220 nm organic membrane, and stored at 4 °C for future use.

#### **Preparation of Pd nanoparticles**

The precursor solution of sodium tetrachloropalladate ( $\text{Na}_2\text{PdCl}_4$ ) was prepared by dissolving 20 mg of  $\text{PdCl}_2$  in 10 mL of sodium chloride solution, followed by stirring at 45 °C until the solution turned deep yellow and clear. The solution was then cooled to room temperature for subsequent use. Separately, ascorbic acid (0.05 g) and PVP (0.03 g) were dissolved in 20 mL of deionized water under ultrasonication. After preheating the solution at 80 °C for 5 minutes, 1 mL of the  $\text{Na}_2\text{PdCl}_4$  solution was added dropwise. The reaction mixture was maintained for 3 hours. The final product was purified by dialysis against ultrapure water for 3 days and then freeze-dried to obtain black Pd NPs in solid form.

#### **Preparation of CPPA nanoparticles**

Dopamine hydrochloride (0.01 g) and Pd NPs (0.01 g) were dissolved in 4 mL of deionized water *via* ultrasonication, followed by the addition of 10 mL of absolute ethanol containing 1 mL of  $\text{CaO}_2$  NPs. The pH was adjusted to approximately 8.5 using 1 M NaOH, and the mixture was stirred in the dark for 12 hours. The resulting black precipitate was collected by centrifugation at 12000 rpm, washed three times with deionized water, and redispersed in 10 mL of deionized water. Sodium phytate (0.01 g) was then added, and the mixture was stirred at room temperature for 24 hours. After washing three times with deionized water, the final product was filtered through a 220 nm membrane.

#### **Preparation of $\text{CaO}_2$ -FITC, and CPPA-FITC nanoparticles**

Appropriate amounts of  $\text{CaO}_2$  NPs or CPPA NPs were dispersed in 15 mL of absolute ethanol and stirred at 600 rpm. Fluorescein isothiocyanate (FITC, 2 mg) was dissolved in 1 mL of absolute ethanol and added dropwise to the nanoparticle suspension. The mixture was stirred at 4 °C for 24 hours to allow for covalent conjugation. The resulting FITC-labeled nanoparticles were collected by centrifugation at 12000 rpm for 20 minutes, washed five times with absolute ethanol, redispersed in 1 mL of absolute ethanol, filtered through a 220 nm membrane, and stored at 4 °C in the dark.

#### **Preparation of $\text{CaO}_2$ -ICG, and CPPA-ICG nanoparticles**

The preparation procedure was identical to that for FITC labeling, except that indocyanine green (ICG) was used as the fluorescent dye.

#### **Photothermal effect and stability of CPPA nanoparticles**

Aqueous solutions of CPPA NPs (200  $\mu\text{L}$ ) were prepared in 1.5 mL Eppendorf tubes at final  $[\text{Ca}^{2+}]$  of 0, 2, 4, 8, and 16  $\mu\text{mol L}^{-1}$ . Each sample was irradiated with either an 808 nm or 1064 nm laser at power densities of 1.0, 1.2, and 1.4  $\text{W cm}^{-2}$  for 10 minutes. The temperature was recorded every 30 seconds using a digital thermometer, and thermal images were acquired at time intervals of 0, 100, 200, 300, 400, 500, and 600 seconds. To investigate photothermal stability, CPPA NP suspensions ( $[\text{Ca}^{2+}] = 8 \mu\text{mol L}^{-1}$ ) were irradiated under either 808 nm or 1064 nm lasers ( $1.2 \text{ W cm}^{-2}$ ) for 10 minutes, followed by natural cooling to room temperature. This heating-cooling cycle was repeated four times to assess repeatability.

Determination of photothermal conversion efficiency (PCE): The PCE of CPPA NPs was calculated based on temperature elevation under continuous laser irradiation (808 or 1064 nm,  $1.2 \text{ W cm}^{-2}$ ) until a thermal steady state was reached, followed by natural cooling. The photothermal conversion efficiency ( $\eta$ ) was calculated according to the following equation:

$$\eta = \frac{hS(T_{\max} - T_{\text{surr}}) - Q_s}{I(1 - 10^{-A_\lambda})}$$

$h$  ( $\text{mW} \cdot \text{m}^{-2} \cdot ^\circ\text{C}^{-1}$ ) is the heat transfer coefficient;  $S$  ( $\text{m}^2$ ) is the surface area of the container;  $T_{\max}$  ( $^\circ\text{C}$ ) is the maximum steady-state temperature;  $T_{\text{surr}}$  ( $^\circ\text{C}$ ) is the ambient temperature;  $Q_s$  ( $\text{mW}$ ) accounts for heat absorbed by the solvent and container;  $I$  is the incident laser power density;  $A_\lambda$  is the absorbance of the CPPA NPs at either 808 or 1064 nm.

### **Extracellular stability of $\text{CaO}_2$ and CPPA nanoparticles**

$\text{CaO}_2$  NPs and CPPA NPs were dispersed in either physiological saline or cell culture medium (10 mL) to obtain nanoparticle suspensions with a final  $\text{Ca}^{2+}$  concentration of 8  $\mu\text{mol L}^{-1}$ . The hydrodynamic diameter and polydispersity index (PDI) were monitored over 7 consecutive days using dynamic light scattering (DLS) to assess their colloidal stability in different extracellular media.

### **pH and Light-dependent $\text{H}_2\text{O}_2$ release from CPPA nanoparticles**

To evaluate pH-responsive  $\text{H}_2\text{O}_2$  release, CPPA NPs were suspended in buffer solutions of varying pH (7.4, 6.5, and 6.0), incubated for 1 hour, and subsequently centrifuged to collect the supernatants. The concentration of released  $\text{H}_2\text{O}_2$  was quantified using a commercial hydrogen peroxide assay kit. For light-responsive release studies, CPPA NPs at various concentrations were dissolved in deionized water and divided into two groups: light-exposed and non-illuminated. After 1 hour of incubation under irradiation or in the dark, the supernatants were collected by centrifugation, and the  $\text{H}_2\text{O}_2$  levels were measured using the same detection assay.

## **Cell culture**

Mouse breast cancer cells (4T1 cells) and mouse pre-osteoblast cells (MC3T3-E1 cells) were purchased from the Cell Bank of the Shanghai Institute of Life Sciences, Chinese Academy of Sciences. 4T1 cells were cultured in Roswell Park Memorial Institute (RPMI) 1640 medium containing 10% fetal bovine serum (FBS) and 1% penicillin-streptomycin (PS), with medium changes every day. MC3T3-E1 cells were cultured in  $\alpha$ -Minimal Essential Medium ( $\alpha$ -MEM) supplemented with 10% FBS and 1% PS, with medium changes every 3 days. All cells were incubated in a standard cell culture incubator at 37 °C with 5% CO<sub>2</sub>. Cells were passaged when they reached 80-90% confluence, using 0.25% trypsin-EDTA for detachment.

## **Osteogenic differentiation and mineralization assay of MC3T3-E1 cells *In vitro***

Preparation of osteogenic induction medium. The osteogenic medium was prepared by supplementing complete  $\alpha$ -MEM with 50 nmol L<sup>-1</sup> ascorbic acid, 10 mmol L<sup>-1</sup>  $\beta$ -glycerophosphate disodium salt, and 100 nmol L<sup>-1</sup> dexamethasone. The components were mixed thoroughly before use. Evaluation of nanoparticle-induced osteogenic differentiation *via* ALP activity. To investigate the effect of nanoparticles on osteogenic differentiation, MC3T3-E1 cells were seeded into 24-well plates at a density of 1×10<sup>5</sup> cells per well. After incubation with treatments for 4 hours, cells in the laser group were irradiated with an 808 nm laser at a power density of 1.2 W cm<sup>-2</sup> for 10 minutes. All groups were then cultured with 500  $\mu$ L per well of osteogenic induction medium for 5 days. Cells cultured with complete  $\alpha$ -MEM served as the negative control, while those treated with osteogenic induction medium alone were used as the positive control. At the end of the induction period, cells were fixed with 4% paraformaldehyde and stained using an alkaline phosphatase (ALP) staining kit. The stained cells were observed and imaged under an upright fluorescence microscope. In accordance with the manufacturer's instructions, ALP activity was quantitatively analyzed using a bicinchoninic acid (BCA) protein assay kit and an ALP activity assay kit.

## **Evaluation of mineralization *via* alizarin red S staining**

To assess matrix mineralization, MC3T3-E1 cells were treated as described above, followed by culture in osteogenic induction medium (500  $\mu$ L per well) for 14 days. After fixation with 4% paraformaldehyde, cells were stained with Alizarin Red S solution (pH 4.2) for 10 minutes, followed by three washes with deionized water. Mineralized nodules were visualized and documented under an upright fluorescence

microscope. To quantify calcium deposition, the bound dye was solubilized using 10% cetylpyridinium chloride, and absorbance was measured at 570 nm to evaluate the degree of mineralization.

#### **Intracellular calcium ion (Ca<sup>2+</sup>) content measurement**

4T1 cells were seeded into 48-well plates at a density of  $5 \times 10^4$  cells per well and incubated at 37 °C for 24 hours. Following treatment according to experimental groups, cells were collected into 15 mL centrifuge tubes and spun down at 1200 rpm for 5 minutes. The cell pellets were resuspended in 1 mL physiological saline and subjected to ultrasonic lysis on ice. The lysates were then centrifuged at 12,000 rpm for 10 minutes at 4 °C. The supernatant was collected, and the absorbance was measured at 575 nm to determine intracellular calcium content.

#### **Detection of mitochondrial calcium overload**

4T1 cells were seeded at a density of  $2 \times 10^4$  cells per well into 35 mm glass-bottom dishes (4-chamber format) and incubated for 24 hours. Cells were then stained with MitoTracker™ Deep Red 633 (100 nM;  $\lambda_{\text{ex}}$ : 622 nm,  $\lambda_{\text{em}}$ : 648 nm) for 20 minutes, followed by three gentle washes with PBS (10 mmol L<sup>-1</sup>, pH 7.4). After designated treatments ( $[\text{Ca}^{2+}] = 8 \mu\text{mol L}^{-1}$ ,  $[\text{PO}_4^{3-}] = 10 \text{ mmol L}^{-1}$ ) for 4 hours, cells in the laser group were irradiated with an 808 nm laser (1.2 W cm<sup>-2</sup>) for 10 minutes and incubated for an additional hour. Cells were then stained with Hoechst 33342 for nuclear visualization and Fluo-4 AM ( $\lambda_{\text{ex}}$ : 494 nm,  $\lambda_{\text{em}}$ : 516 nm) to assess intracellular Ca<sup>2+</sup> levels, and imaged using confocal laser scanning microscopy (CLSM).

#### **Detection of intracellular reactive oxygen species (ROS)**

4T1 cells were seeded in 48-well plates at  $5 \times 10^4$  cells per well and incubated for 24 hours. After designated treatments ( $[\text{Ca}^{2+}] = 8 \mu\text{mol L}^{-1}$ ,  $[\text{PO}_4^{3-}] = 10 \text{ mmol L}^{-1}$ ) for 4 hours, cells in the laser group were irradiated with an 808 nm laser (1.2 W cm<sup>-2</sup>) for 10 minutes, followed by a 24-hour incubation. Cells were then washed three times with PBS (10 mmol L<sup>-1</sup>, pH 7.4) and stained with DCFH-DA to visualize intracellular ROS levels using an inverted fluorescence microscope.

#### **Apoptosis detection**

4T1 cells were seeded into 24-well plates at a density of  $1 \times 10^5$  cells per well and incubated for 24 hours. Following treatment according to the experimental groups, cells were further cultured for 4 hours. For the laser-treated group, cells were exposed to an 808 nm laser at a power density of 1.2 W cm<sup>-2</sup> for 10 minutes, followed by an additional 24-hour incubation. Subsequently, cells were gently washed three

times with PBS (10 mmol L<sup>-1</sup>, pH 7.4), stained using an apoptosis detection kit, and analyzed by flow cytometry.

### **3D tumor spheroid assay**

Tumor spheroid penetration: 4T1 cells were seeded at 5,000 cells per well in BexgGold™ ultra-low attachment 96-well plates and cultured for 24–48 hours until the spheroids reached a diameter of approximately 500 μm. FITC-labeled CaO<sub>2</sub> nanoparticles (NPs) and CPPA NPs were co-incubated with the spheroids for 4, 8, 12, and 24 hours. After incubation, the medium was carefully removed, and the spheroids were gently washed twice with PBS. Tumor spheroid penetration at various depths was assessed and imaged using a laser scanning confocal microscope.

Tumor spheroid calcification: Spheroids were incubated with the designated treatments for 24 hours in the presence of [Ca<sup>2+</sup>] (8 μmol L<sup>-1</sup>) and [PO<sub>4</sub><sup>3-</sup>] (10 mmol L<sup>-1</sup>). For the laser group, spheroids were irradiated with an 808 nm laser at a power density of 1.2 W cm<sup>-2</sup> for 10 minutes, followed by an additional 24-hour incubation. Afterward, spheroids were gently washed three times with PBS (10 mmol L<sup>-1</sup>, pH 7.4), and nuclei were stained with Hoechst 33342. Calcified regions were stained with calcein ( $\lambda_{\text{ex}} = 495$  nm,  $\lambda_{\text{em}} = 515$  nm), and imaging was performed using a laser scanning confocal microscope.

### **Establishment of a mouse model for breast cancer bone metastasis**

Balb/c mice were randomly divided into four groups (n = 15): PBS, CaO<sub>2</sub>, CPPA, and CPPA + L (with CaO<sub>2</sub> concentration set at 8 μmol). Once the mice reached approximately 19 g, the model was initiated by direct injection of 4T1 cells into the right tibia to establish the breast cancer bone metastasis model. The procedure was as follows: First, Balb/c mice were anesthetized with inhaled isoflurane. A small hole was drilled into the right tibia using a skull drill, and 10 μL of a 4T1 cell suspension (2.5 × 10<sup>5</sup> cells, mixed with Matrigel in a 2:1 ratio) was injected into the tibia using a micro-syringe. After suturing, the wound was treated with erythromycin ointment to prevent infection, and erythromycin ointment was applied every other day during the observation period. After model establishment, mice exhibited normal activity and feeding behavior.

### ***In vivo* bone targeting ability assessment**

An orthotopic breast cancer bone metastasis model was established in the right tibia of Balb/c mice. Once the tumor reached approximately 200 mm<sup>3</sup>, fluorescence imaging was performed. Mice were randomly divided into two groups and intravenously injected with either CaO<sub>2</sub>-ICG NPs or CPPA-ICG NPs ([Ca<sup>2+</sup>] = 8 μmol L<sup>-1</sup>) suspended in 200 μL. Fluorescence imaging was performed at time points of

0, 2, 4, 8, 12, and 24 hours post-injection to monitor nanoparticle accumulation at the tumor site. After determining the time point with maximum nanoparticle accumulation, mice were euthanized, and their organs (heart, liver, spleen, lungs, kidneys, and tumor-bearing tibia) were dissected for fluorescence imaging.

#### ***In vivo* photothermal performance assessment**

To evaluate the photothermal properties of CPPA NPs in Balb/c mice, the optimal nanoparticle accumulation time at the tumor site was determined using fluorescence imaging. After intravenous injection of CPPA NPs ( $[Ca^{2+}] = 8 \mu\text{mol L}^{-1}$ ), the tumor area was irradiated with an 808 nm laser ( $1.2 \text{ W cm}^{-2}$ ) for 10 minutes at the optimal time point. Real-time temperature changes were recorded using an infrared thermal imaging system during both the first and second treatments (separated by 6 days).

#### ***In vivo* evaluation of breast cancer inhibition**

Four days post-injection of 4T1 cells, treatment was administered (intravenous injection of PBS,  $\text{CaO}_2$ , or CPPA). After 8 hours, the right leg tumor site was irradiated with an 808 nm laser ( $1.2 \text{ W cm}^{-2}$ ) for 10 minutes, while temperature changes in the tumor area were recorded using thermal imaging. The treatment regimen consisted of two injections and laser exposures (on Day 0 and Day 6). Mice were weighed, and tumor volumes were measured every other day. After 14 days of treatment, mice were euthanized under isoflurane anesthesia, and major organs (heart, liver, spleen, lungs, kidneys) as well as the right leg tibia tumor were harvested for histopathological analysis. The tissues were fixed in 4% paraformaldehyde for 24 hours. The calcification of the right tibia tumor was assessed using micro-CT, and bone-related parameters (BV/TV, BS/BV, Tb.Sp, BMD) were measured. Additionally, the right tibia tumor tissue was subjected to H&E staining, Ki67, TUNEL, and Alizarin Red S (ARS) staining. Blood was collected for hematological and biochemical analysis to assess biosafety. Finally, tumor samples were sent for transcriptome sequencing.

#### **Cellular uptake of $\text{CaO}_2$ and CPPA nanoparticles**

Once MC3T3-E1 or 4T1 cells in culture flasks reached 80-90% confluence, they were seeded into four-well 35 mm glass-bottomed culture dishes at a density of  $2 \times 10^4$  cells per well. The cells were then co-cultured with CPPA-FITC NPs ( $[Ca^{2+}] = 8 \mu\text{mol L}^{-1}$ ) for 2, 4, 8, 12, and 24 hours. After incubation, the cells were fixed with 4% paraformaldehyde at  $4^\circ\text{C}$  for 15 minutes. Following three washes with PBS ( $10 \text{ mmol L}^{-1}$ ,  $\text{pH} = 7.4$ ), the cell nuclei were stained with Hoechst 33342 ( $1 \mu\text{L}$ ) for 20 minutes.

Afterward, cells were washed again with PBS and the uptake of nanoparticles was observed using laser scanning confocal microscopy.

### **Biocompatibility evaluation**

Cells were seeded into 96-well plates at a density of  $8 \times 10^3$  cells per well. After 24 hours of incubation, CPPA NPs solutions at different  $[\text{Ca}^{2+}]$  (0, 0.5, 1, 2, 4, 8, and  $16 \mu\text{mol L}^{-1}$ ) were added, and the cells were further cultured for 24 hours. After discarding the original medium, 0.5 mg/mL MTT solution was added to each well, and the cells were incubated for an additional 4 hours. The supernatant was then discarded, and 150  $\mu\text{L}$  of dimethyl sulfoxide (DMSO) was added to dissolve the formazan crystals. The absorbance at 490 nm was measured using a microplate reader, and relative cell viability was calculated using the following formula: cell viability (%) =  $(\text{OD}_{\text{sample}} - \text{OD}_{\text{blank control}}) / (\text{OD}_{\text{control}} - \text{OD}_{\text{blank control}}) \times 100\%$ .

### **Cytotoxicity evaluation**

Cells were seeded in 48-well plates at a density of  $5 \times 10^4$  cells per well and incubated at 37 °C for 24 hours. After treatment according to the respective experimental groups, cells were further cultured for 4 hours (with  $[\text{Ca}^{2+}] = 8 \mu\text{mol L}^{-1}$  and  $[\text{PO}_4^{3-}] = 10 \text{ mmol L}^{-1}$ ). The laser group was irradiated with an 808 nm laser at a power density of  $1.2 \text{ W cm}^{-2}$  for 10 minutes, followed by 1 hour of additional incubation. Afterward, cells were gently washed once with PBS ( $10 \text{ mmol L}^{-1}$ , pH = 7.4) and stained with a live/dead cell viability kit for 20 minutes. After staining, cells were washed once with PBS, and 200  $\mu\text{L}$  of complete culture medium was added to each well. Cell viability was observed under an inverted fluorescence microscope to assess live/dead cell status.

### **Mitochondrial membrane potential assessment**

4T1 cells were seeded at a density of  $2 \times 10^4$  cells per well into 35 mm glass-bottom dishes with four chambers. After treatment with nanoparticles for 4 hours ( $[\text{Ca}^{2+}] = 8 \mu\text{mol L}^{-1}$ ,  $[\text{PO}_4^{3-}] = 10 \text{ mmol L}^{-1}$ ), cells in the laser group were irradiated with an 808 nm laser ( $1.2 \text{ W cm}^{-2}$ ) for 10 minutes, followed by an additional 1 hour of incubation. Mitochondrial membrane potential was then analyzed using the JC-1 assay kit. Cells were incubated with JC-1 working solution for 20 minutes, washed with JC-1 buffer solution, and imaged by confocal laser scanning microscopy (CLSM). Green fluorescence ( $\lambda_{\text{em}}$ : 510–540 nm) indicated JC-1 monomers, reflecting mitochondrial depolarization, while red fluorescence ( $\lambda_{\text{em}}$ : 570–620 nm) represented JC-1 aggregates, indicating intact mitochondrial membrane potential.

### **Cell migration assay**

4T1 cells were seeded at a density of  $1 \times 10^5$  cells per well in 24-well plates and incubated for 24 hours. A 200  $\mu\text{L}$  sterile pipette tip was fitted onto a 1 mL pipette and used to create a scratch approximately 0.5 mm wide at the bottom of each well. After administration of the respective treatments, cells were incubated for an additional 4 hours. For the laser-treated group, cells were irradiated with an 808 nm laser ( $1.2 \text{ W cm}^{-2}$ ) for 10 minutes and further incubated for 24 or 48 hours. The medium was then removed, and cells were washed three times with PBS. Three random fields per well were imaged under a microscope. Cell migration was quantified by analyzing the number of cells that had moved into the scratched area.

### **Assessment of cell calcification**

Alizarin red S staining of calcified nodules. To assess mineral deposition, 4T1 cells were seeded into 24-well plates at  $1 \times 10^5$  cells per well. After 4 hours of treatment ( $[\text{Ca}^{2+}] = 8 \mu\text{mol L}^{-1}$ ,  $[\text{PO}_4^{3-}] = 10 \text{ mmol L}^{-1}$ ), cells in the laser group were irradiated with an 808 nm laser ( $1.2 \text{ W cm}^{-2}$ ) for 10 minutes and further incubated for 24 hours. Cells were washed with PBS, fixed with 4% paraformaldehyde, and stained with Alizarin Red S solution (pH 4.2) for 10 minutes. After three washes with deionized water, calcium deposits were imaged under an upright fluorescence microscope. Bound dye was solubilized in 10% cetylpyridinium chloride, and absorbance was measured at 570 nm to quantify the degree of calcification.

Fluorescent localization of membrane calcification. To visualize membrane-associated calcification, 4T1 cells were seeded at  $2 \times 10^4$  cells per well in 4-chamber 35 mm glass-bottom dishes. Prior to treatment, cells were incubated with DiD ( $10 \mu\text{mol L}^{-1}$ ;  $\lambda_{\text{ex}}$ : 644 nm,  $\lambda_{\text{em}}$ : 665 nm) for 20 minutes and washed three times with PBS. Cells were then treated ( $[\text{Ca}^{2+}] = 8 \mu\text{mol L}^{-1}$ ,  $[\text{PO}_4^{3-}] = 10 \text{ mmol L}^{-1}$ ) for 4 hours, irradiated with an 808 nm laser ( $1.2 \text{ W cm}^{-2}$ ) for 10 minutes, and incubated for an additional 24 hours. Hoechst 33342 was used for nuclear staining, and Calcein ( $\lambda_{\text{ex}}$ : 495 nm,  $\lambda_{\text{em}}$ : 515 nm) was applied to label calcified membrane regions. Images were acquired using CLSM.

Scanning electron microscopy (SEM) of membrane calcification. Sterile 13 mm coverslips were placed in 24-well plates, and 4T1 cells were seeded at  $1 \times 10^5$  cells per well. After 24 hours of culture and treatment (including laser irradiation as above), cells were washed and fixed with 2.5% glutaraldehyde for 2 hours at room temperature. Dehydration was performed using graded ethanol series (10%, 30%, 50%, 70%, 90%, and 100%), each for 30 minutes. Samples were air-dried and prepared for SEM imaging.

Analysis of membrane calcification composition *via* fourier transform infrared spectroscopy (FTIR). 4T1 cells were seeded into 24-well plates at a density of  $1 \times 10^5$  cells per well and incubated for 24 hours. After treatment according to experimental groups, including laser irradiation at 808 nm ( $1.2 \text{ W cm}^{-2}$ ) for 10 minutes, cells were further incubated for 24 hours. Following three gentle washes with PBS ( $10 \text{ mmol L}^{-1}$ , pH 7.4), cells were collected using a cell scraper, transferred into centrifuge tubes, and pelleted by centrifugation. The cell pellets were dried in an oven and subsequently subjected to FTIR spectroscopy to analyze the chemical composition of membrane-associated calcification.

### **Hemolysis assay**

Whole blood (1 mL) was collected from non-model Balb/c mice, washed with PBS (pH 7.4), and centrifuged at 3000 rpm for 5 minutes. The red blood cells were collected and diluted with PBS to a final concentration of 2%. A 0.5 mL aliquot of red blood cell suspension was mixed with 0.5 mL of CPPA NPs at varying  $\text{Ca}^{2+}$  concentrations ( $[\text{Ca}^{2+}] = 2, 4, 8, 16, \text{ and } 32 \mu\text{M}$ , respectively), as well as negative (PBS) and positive (deionized water) controls. The mixture was incubated at  $37 \text{ }^\circ\text{C}$  for 2 hours, followed by centrifugation at 10,000 rpm for 5 minutes to collect the supernatant. Hemolysis was quantified by measuring the absorbance at 541 nm using a microplate reader. The hemolysis rate was calculated using the following formula:

$$\text{Hemolysis rate} = (\text{OD}_{\text{sample}} - \text{OD}_{\text{negative control}}) / (\text{OD}_{\text{positive control}} - \text{OD}_{\text{negative control}}) \times 100\%$$

### **Statistical analysis**

All experiments were repeated three times, and data are presented as mean  $\pm$  standard deviation (SD). Statistical differences in means were evaluated using one-way analysis of variance (ANOVA), followed by post hoc comparisons with the least significant difference (LSD) method in SPSS 27.0 software. Statistical significance was indicated as follows: \* $P < 0.05$ , \*\* $P < 0.01$  and \*\*\* $P < 0.001$ .

## Supporting figures

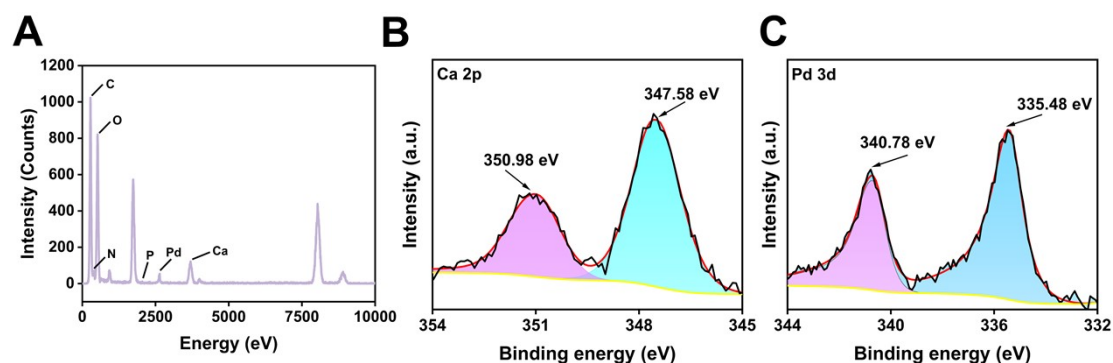


**Figure S1.** (A) EDS analysis of CPPA NPs. High-resolution XPS spectra for Ca 2p (B) and Pd 3d (C) of CPPA NPs.

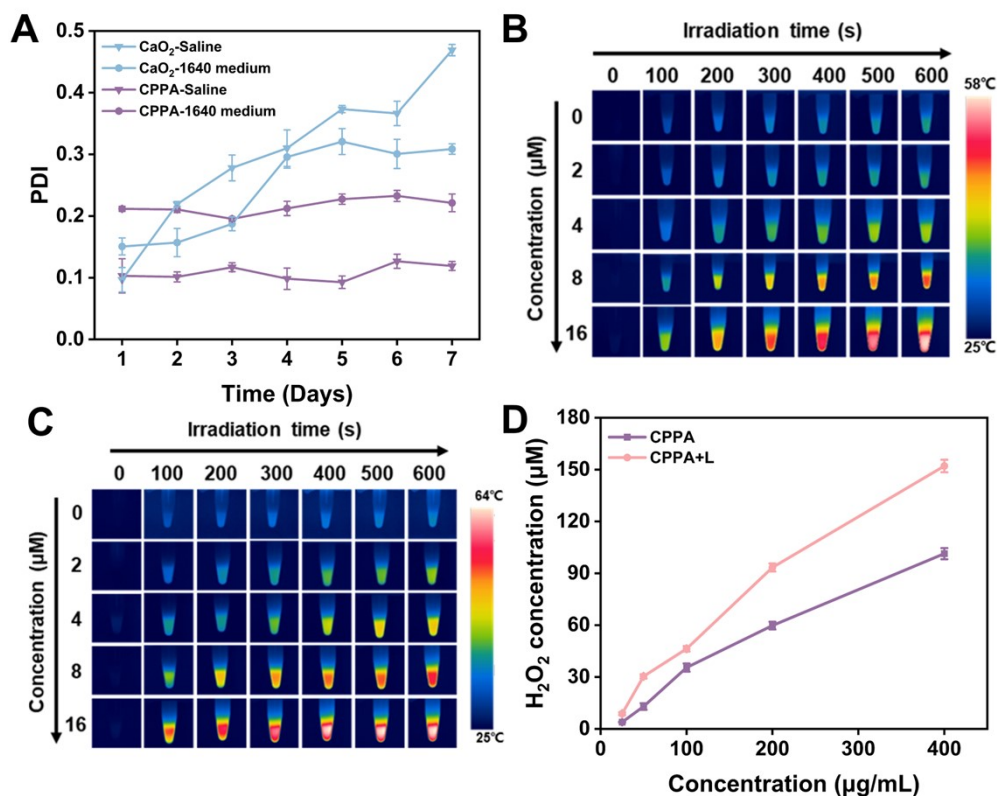


**Figure S2.** (A) The PDI changes of CPPA, CaO<sub>2</sub> NPs within 7 days in PBS and cell culture medium (n=3). (B) IR thermal images of CPPA with different concentrations under irradiation of 1064 nm laser at the power density of 1.2 W cm<sup>-2</sup> for 600 s. (C) IR thermal images of CPPA with different concentrations under irradiation of 808 nm laser at the power density of 1.2 W cm<sup>-2</sup> for 600 s. (D) H<sub>2</sub>O<sub>2</sub> concentration produced under different concentrations of CPPA NPs.

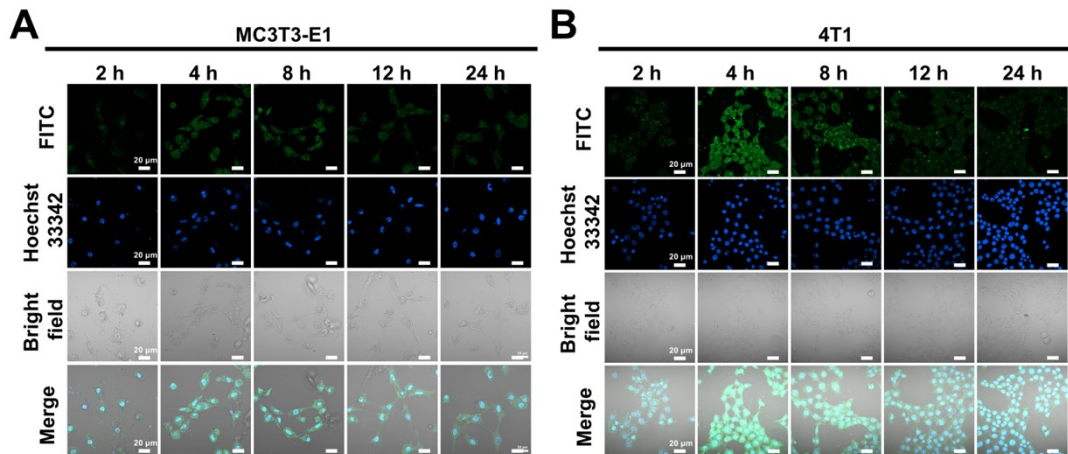


**Figure S3.** (A) CLSM images of MC3T3-E1 cells after incubation with CPPA NPs ( $[Ca^{2+}] = 4 \mu\text{mol L}^{-1}$ ) for different times. Scale bar: 20  $\mu\text{m}$ . (B) CLSM images of 4T1 cells after incubation with CPPA NPs ( $[Ca^{2+}] = 4 \mu\text{mol L}^{-1}$ ) for different times. Scale bar: 20  $\mu\text{m}$ .

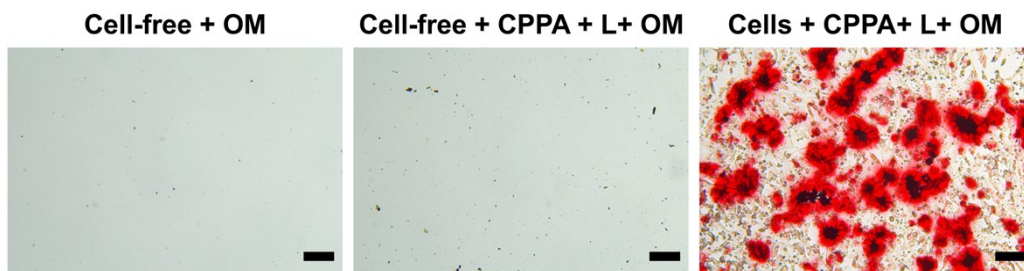


**Figure S4.** Alizarin Red S (ARS) staining was employed to assess mineralization in MC3T3-E1 cells following the specified treatments. Three experimental groups were defined: (i) cell-free with osteogenic medium (Cell-free + OM), (ii) cell-free with CPPA nanoparticles and laser irradiation in conjunction with osteogenic medium (Cell-free + CPPA + L + OM), and (iii) cells with CPPA nanoparticles and laser irradiation in conjunction with osteogenic medium (Cells + CPPA + L + OM). Scale bar: 100  $\mu\text{m}$ . The laser pump powers were 808 nm 1.2 W  $\text{cm}^{-2}$ .

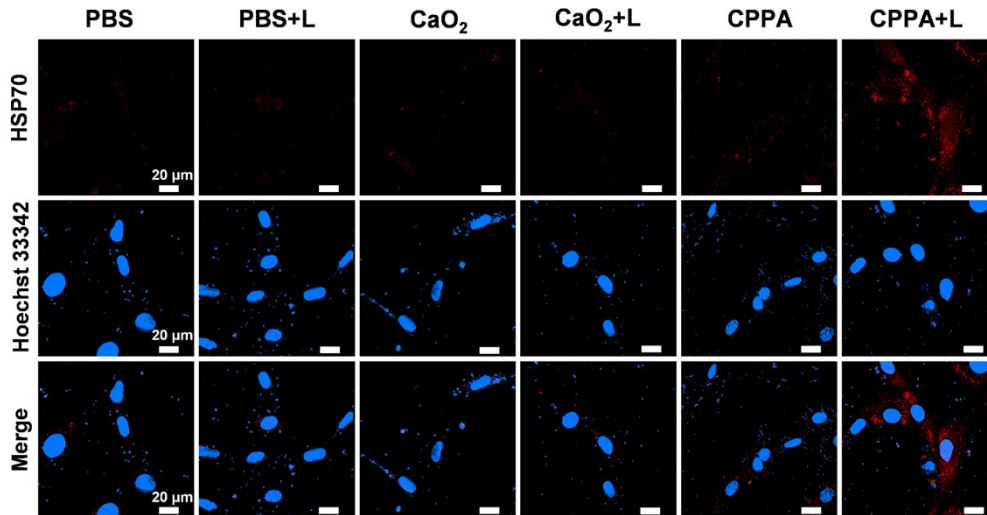


**Figure S5.** CLSM images of MC3T3-E1 cells with immunofluorescence staining of HSP70 after different treatments for 24 h; Scale bars: 20  $\mu\text{m}$ . The laser pump powers were 808 nm 1.2 W  $\text{cm}^{-2}$ .

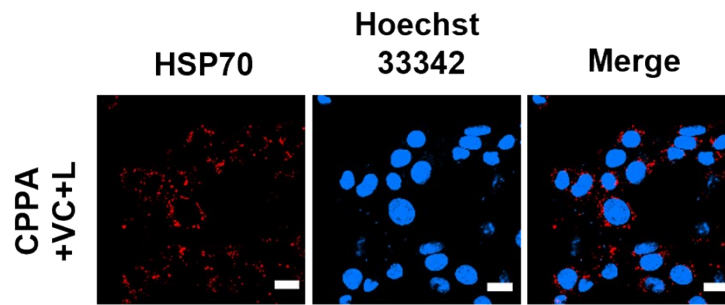


**Figure S6.** CLSM images of 4T1 cells with immunofluorescence staining of HSP70 after different treatments for 24 h; Scale bars: 20  $\mu\text{m}$ .

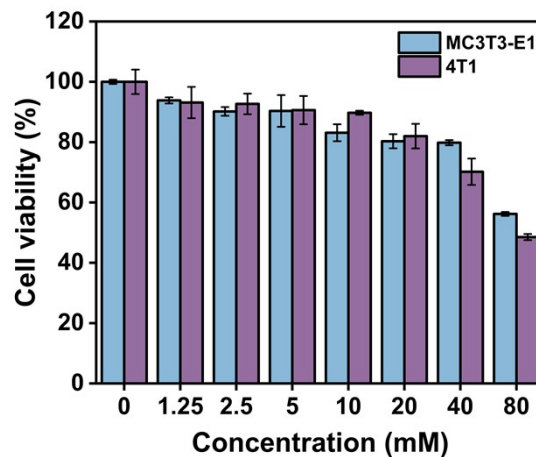


**Figure S7.** The cell viability of 4T1, MC3T3-E1 cells incubated with different concentrations of  $\text{PO}_4^{3-}$  NPs for 24 h.

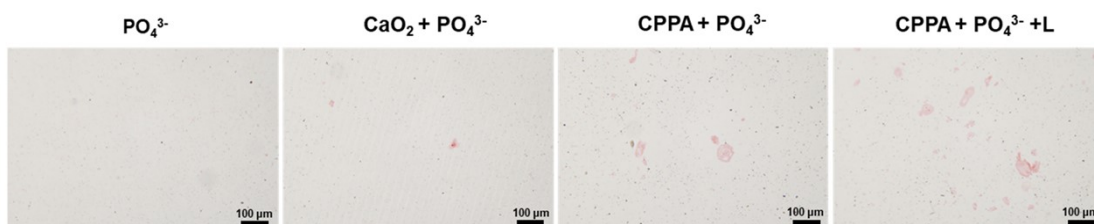


**Figure S8.** CPPA NPs from different groups were incubated for 24 hours under conditions without 4T1 cells and stained with alizarin red. Scale bars: 100  $\mu\text{m}$ .

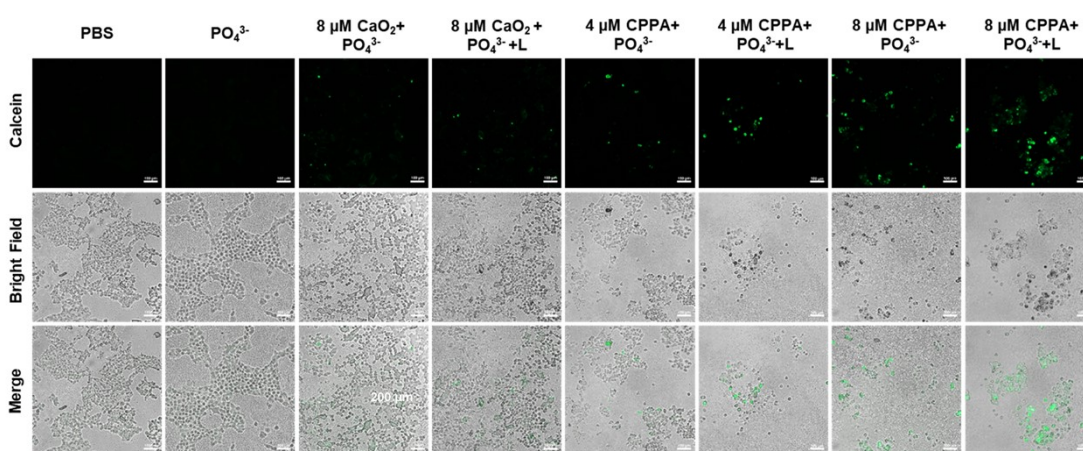


**Figure S9.** Calcein staining of 4T1 cells after different treatments ( $[\text{PO}_4^{3-}] = 10 \text{ mmol L}^{-1}$ ). Scale bar: 20  $\mu\text{m}$ . The laser pump powers were 808 nm  $1.2 \text{ W cm}^{-2}$ .

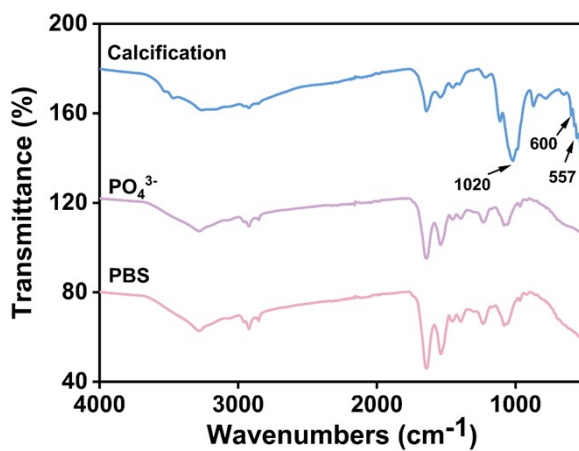


**Figure S10.** FT-IR spectra of 4T1 cells after different treatments.

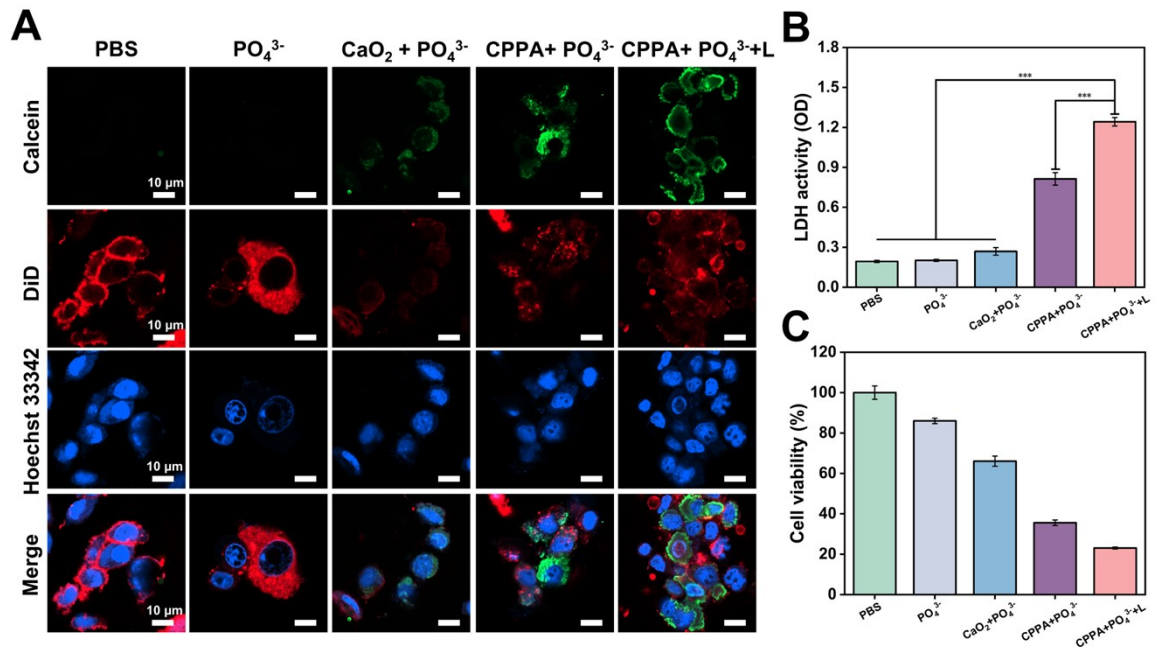


**Figure S11.** (A) Calcein staining of 4T1 cells after different treatments ( $[\text{PO}_4^{3-}] = 10 \text{ mmol L}^{-1}$ ). Scale bar: 20  $\mu\text{m}$ . (B) LDH activity in the medium for 4T1 cells after different treatments ( $[\text{Ca}^{2+}] = 8 \text{ }\mu\text{mol L}^{-1}$ ,  $[\text{PO}_4^{3-}] = 10 \text{ mmol L}^{-1}$ ). (C) Cell viability of 4T1 cells treated with different groups as detected by the MTT assay. The laser pump powers were 808 nm 1.2 W  $\text{cm}^{-2}$ .

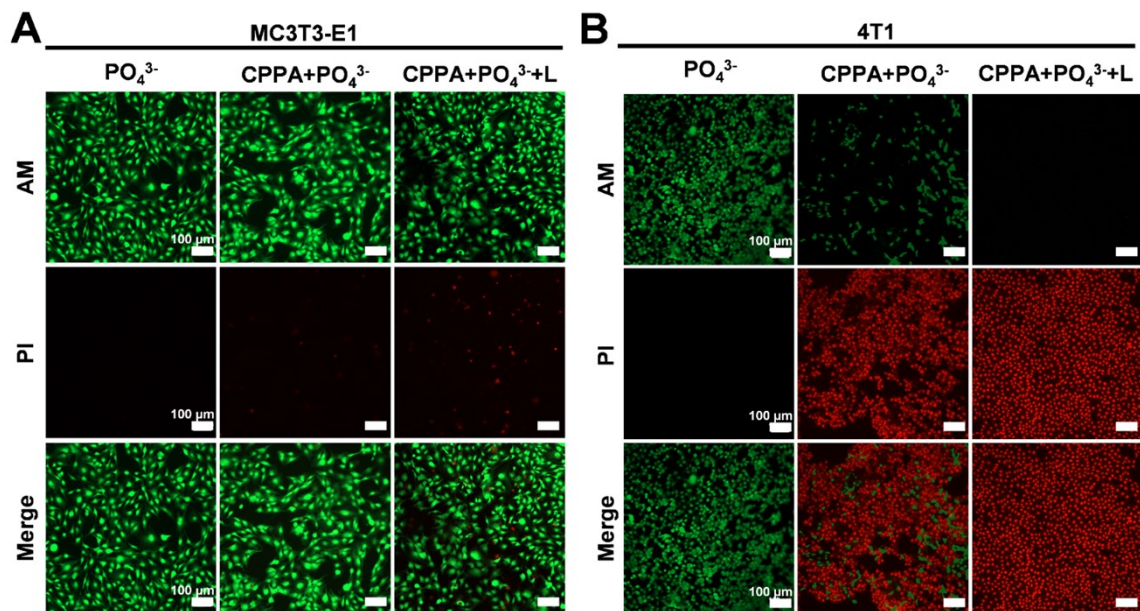


**Figure S12.** Representative Calcein and AM/PI staining of MC3T3-E1 and 4T1 cells following different treatments. Scale bar: 100  $\mu\text{m}$ . The laser pump powers were 808 nm 1.2 W  $\text{cm}^{-2}$ .

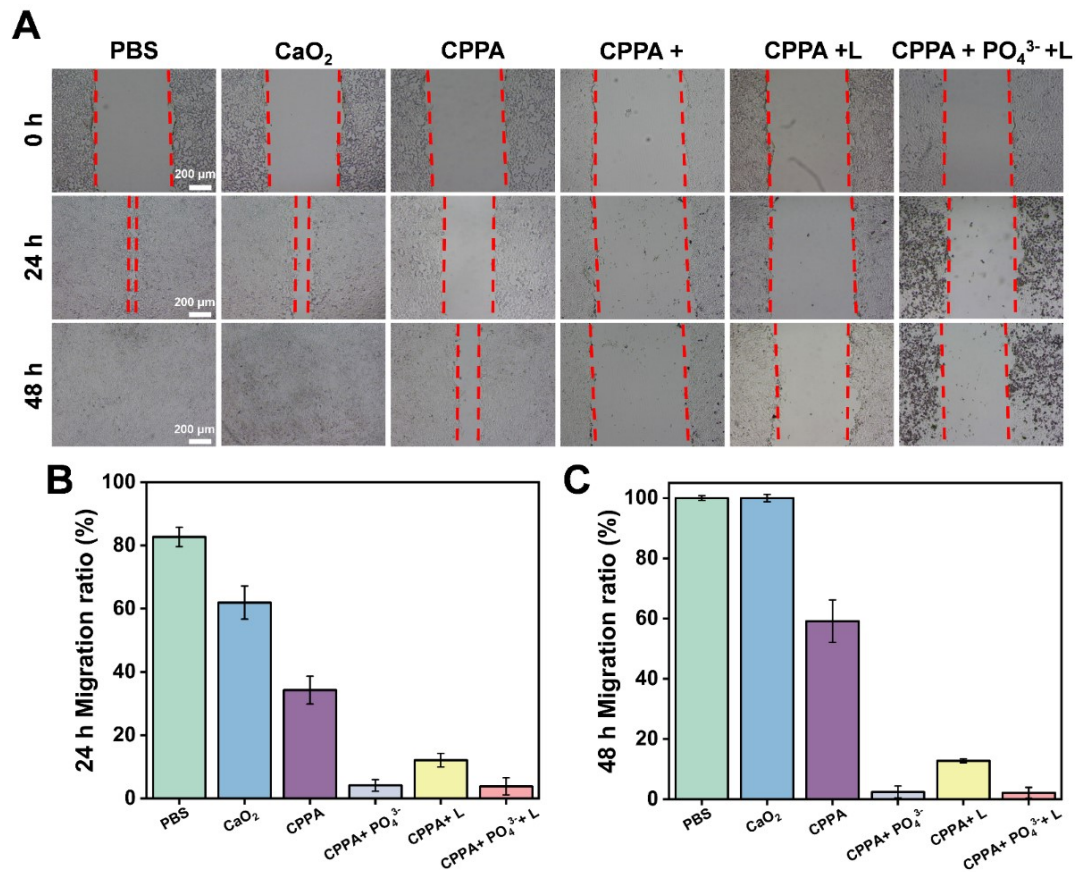


**Figure S13.** (A) Migration images of 4T1 cells after different treatments at 24 h and 48 h, Scale bar: 500  $\mu\text{m}$ ; Migration images of 4T1 cells after different treatments at 24 h (B) and 48 h (C). The laser pump powers were 808 nm 1.2 W  $\text{cm}^{-2}$ .

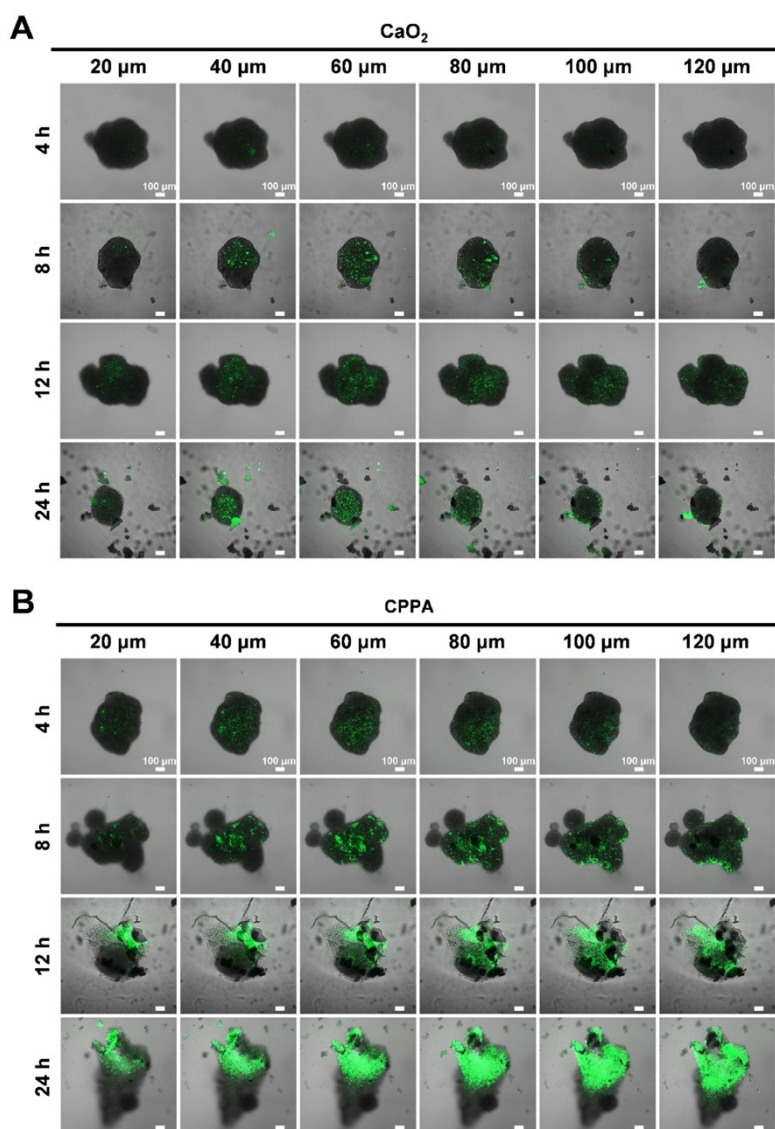


**Figure S14.** CLSM images of 4T1 tumor balls after incubation with  $\text{CaO}_2$  NPs (A) and CPPA NPs (B) ( $[\text{Ca}^{2+}] = 8 \mu\text{mol L}^{-1}$ ) for different times.

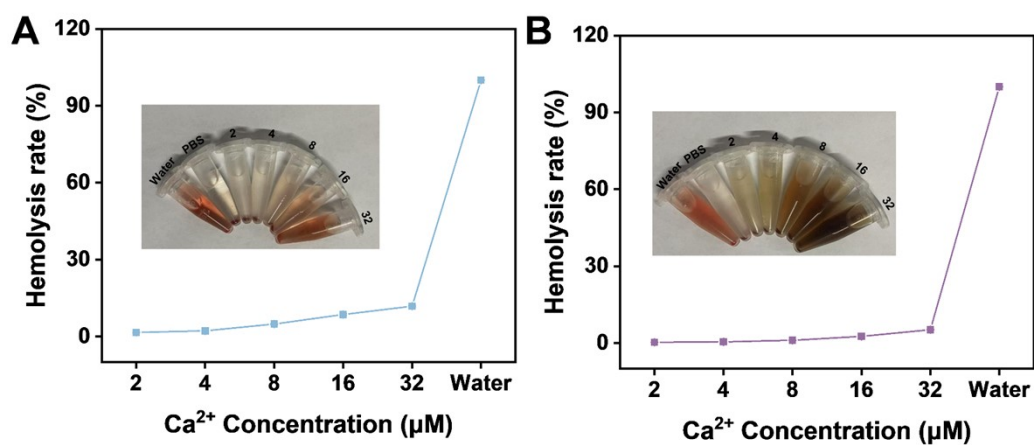


**Figure S15.** Hemolysis rates of (A)  $\text{CaO}_2$  NPs and (B) CPPA NPs at different  $\text{Ca}^{2+}$  concentrations ( $[\text{Ca}^{2+}] = 2, 4, 8, 16, \text{ and } 32 \mu\text{mol L}^{-1}$ ).

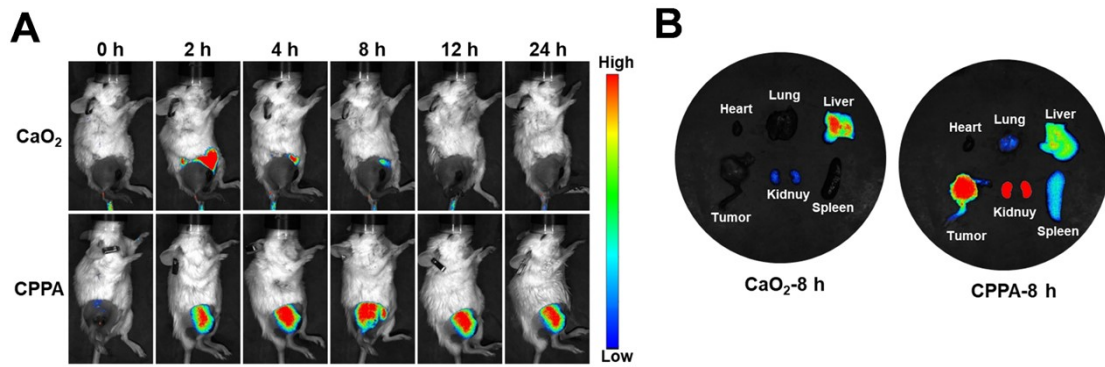


**Figure S16.** (A) Fluorescence images of mice after intravenous injection with ICG labeled CaO<sub>2</sub> and CPPA NPs for different times. (B) Biological distribution of CaO<sub>2</sub> and CPPA nanoparticles labeled with ICG for 8 hours in mouse organs.

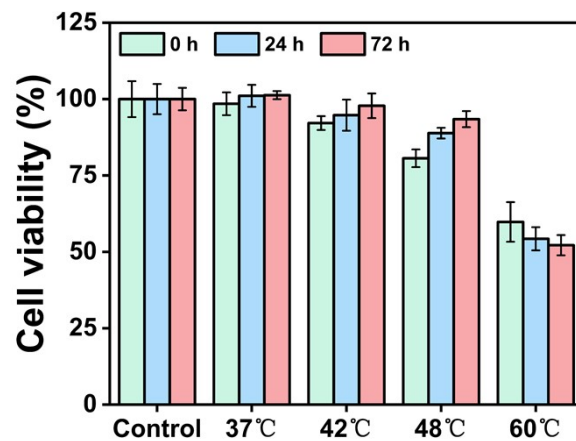


**Figure S17.** Relative viability of MC3T3-E1 cells after exposure to different temperatures, observed at 0, 24, and 72 hours.

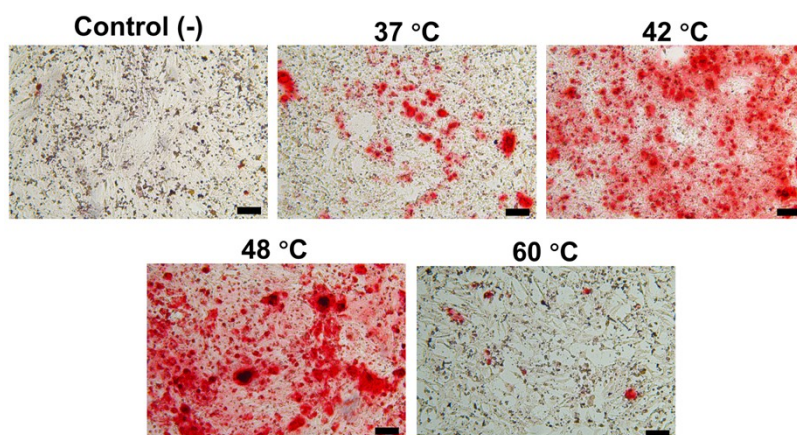


**Figure S18.** Representative images of Alizarin Red S (ARS) staining in MC3T3-E1 cells after 14 days of exposure to different temperatures; Scale bars: 100  $\mu$ m.

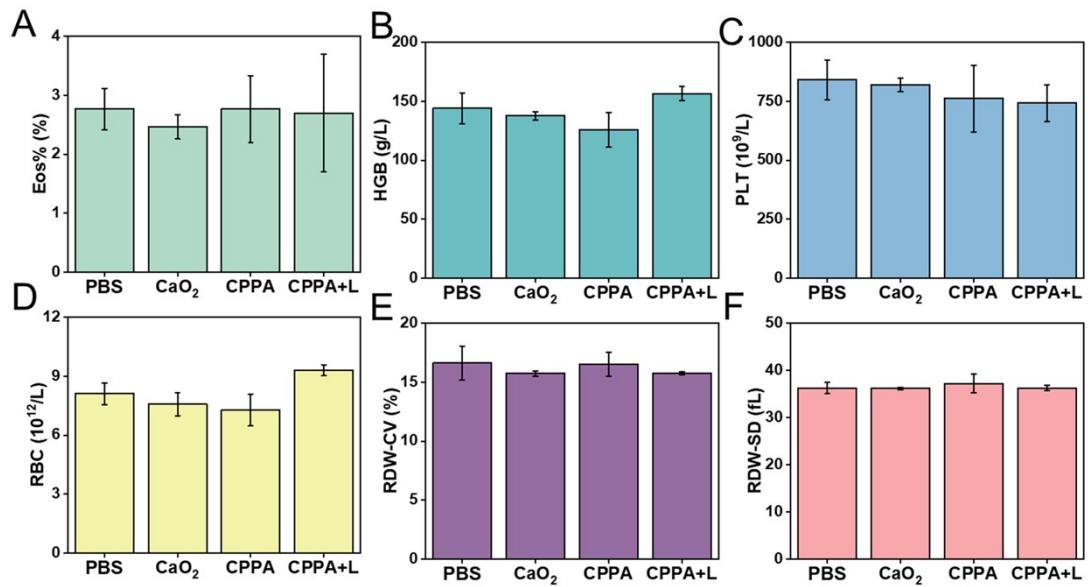


**Figure S19.** Complete blood tests of mice from different groups after 14 days of treatment (A: Eos%; B: HGB; C: PLT; D: RBC; E: RDW-CV; F: RDW-SD).

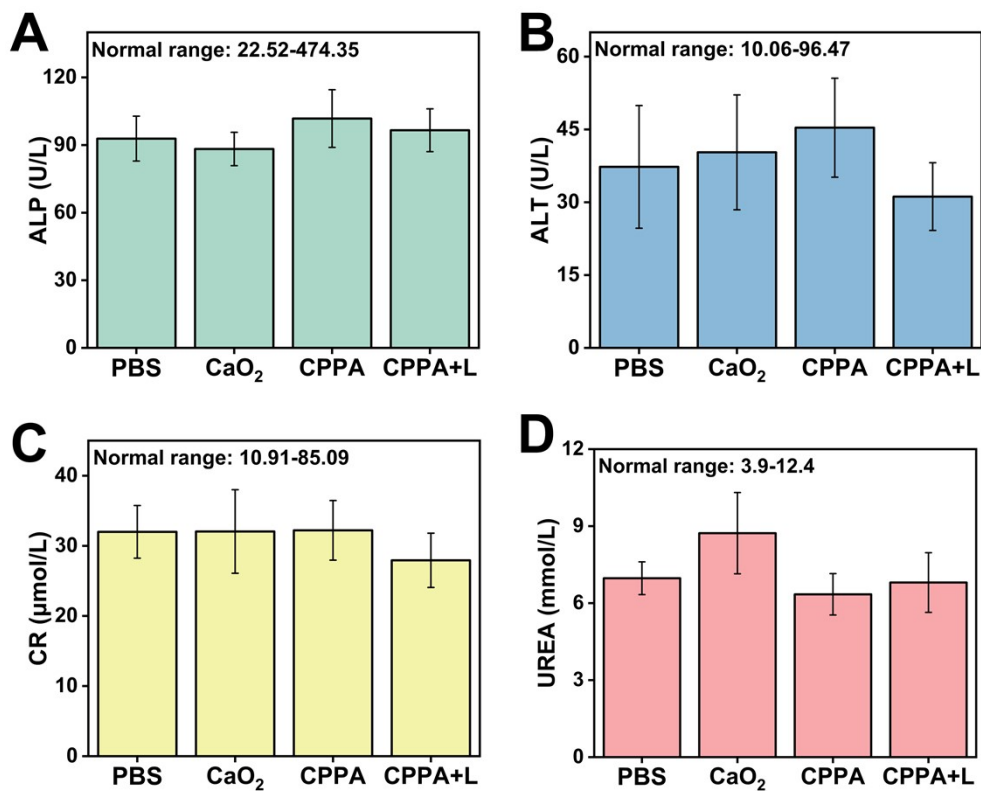


**Figure S20.** Serum tests of mice from different groups after 14 days of treatment (A: ALP; B: ALT; C: CR; D: UREA).

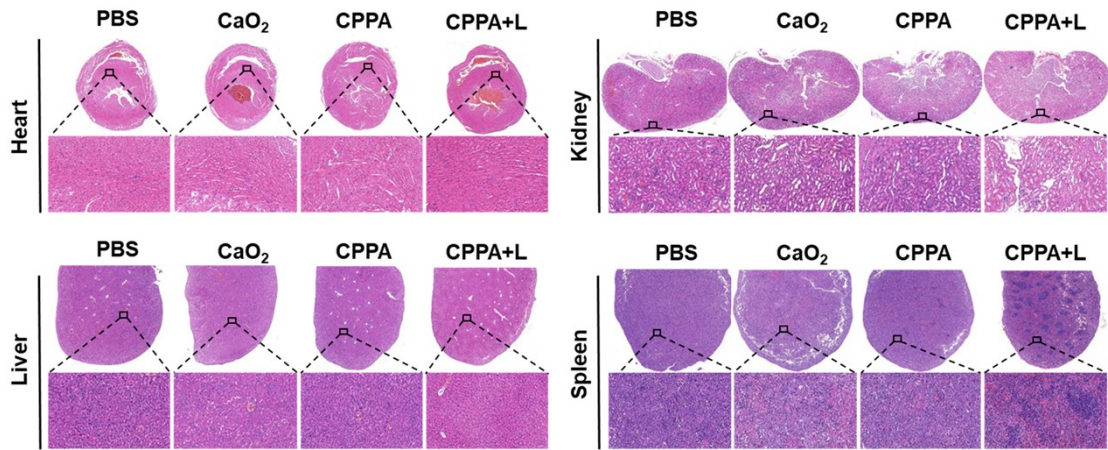


**Figure S21.** Representative H&E-stained histological images of major organs from mice in each group after treatment, in the following order: heart, kidney, liver, and spleen. The scale bars represent 1 mm (top) and 50  $\mu\text{m}$  (bottom).

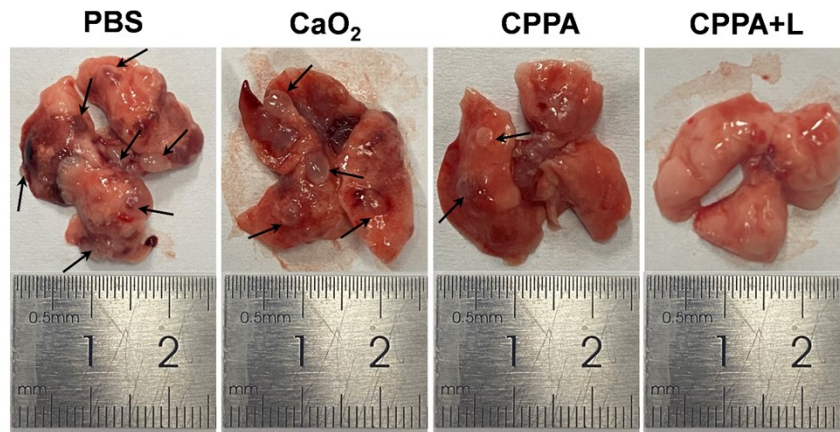


**Figure S22.** Photographs of metastasis nodules in Lung with different treatments. Arrows indicate pulmonary metastatic nodules.

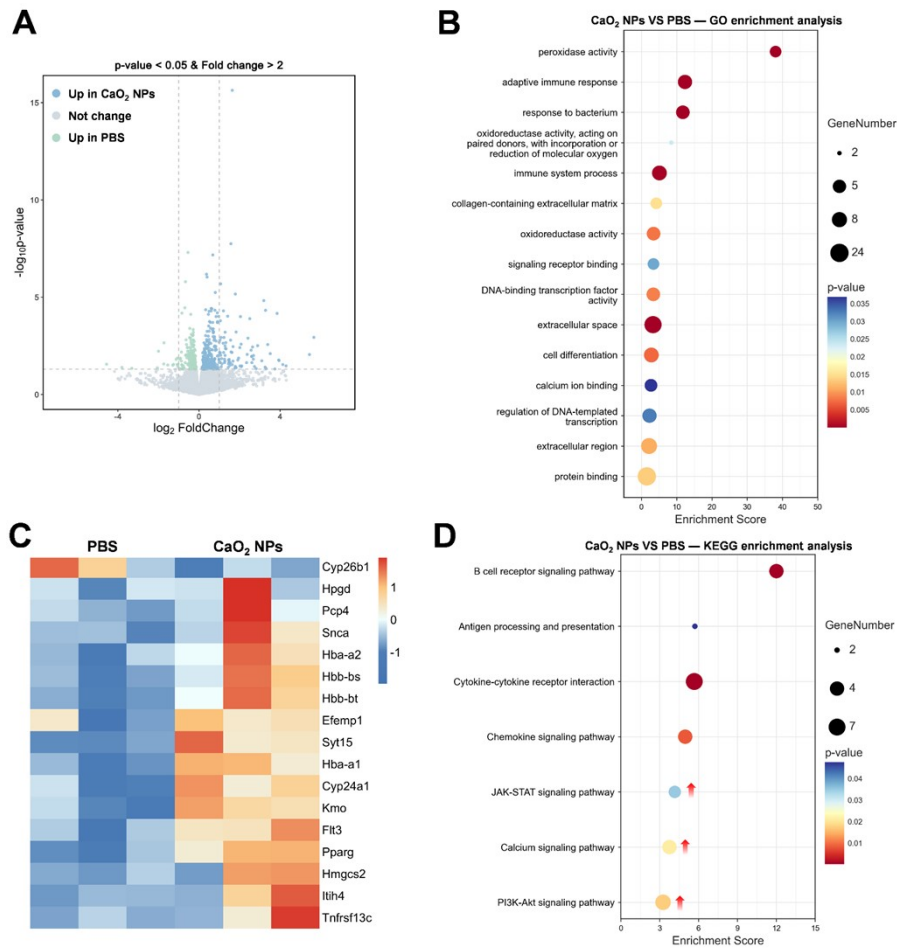


**Figure S23.** (A) Volcano plots of the up-regulated or down-regulated gene in CaO<sub>2</sub> NPs-PBS comparison. (B) KEGG pathway enrichment analyses were performed on differentially expressed genes (DEGs) from tumor tissues between the CaO<sub>2</sub> NPs and PBS groups. (C) Heatmap displaying the expression profiles of DEGs identified between the CaO<sub>2</sub> NPs and PBS groups. (D) Heatmap displaying the expression profiles of DEGs identified between the CaO<sub>2</sub> NPs and PBS groups.

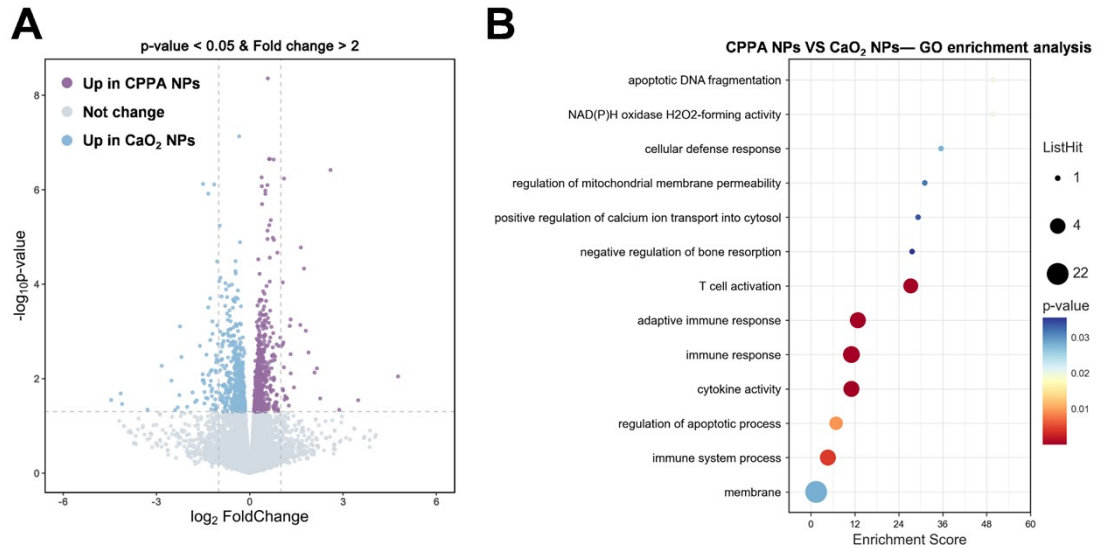


**Figure S24.** (A) Volcano plots of the up-regulated or down-regulated gene in CPPA NPs-CaO<sub>2</sub> NPs comparison. (B) KEGG pathway enrichment analyses were performed on differentially expressed genes (DEGs) from tumor tissues between the CPPA NPs and CaO<sub>2</sub> groups.

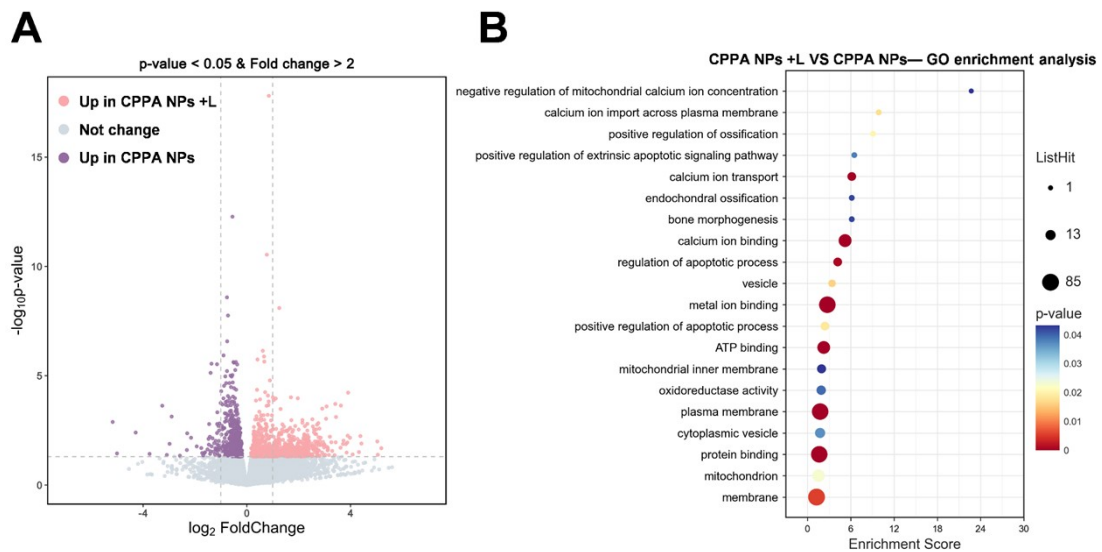


**Figure S25.** (A) Volcano plots of the up-regulated or down-regulated gene in CPPA NPs +L-CPPA NPs comparison. (B) KEGG pathway enrichment analyses were performed on differentially expressed genes (DEGs) from tumor tissues between the CPPA NPs +L and CPPA groups.

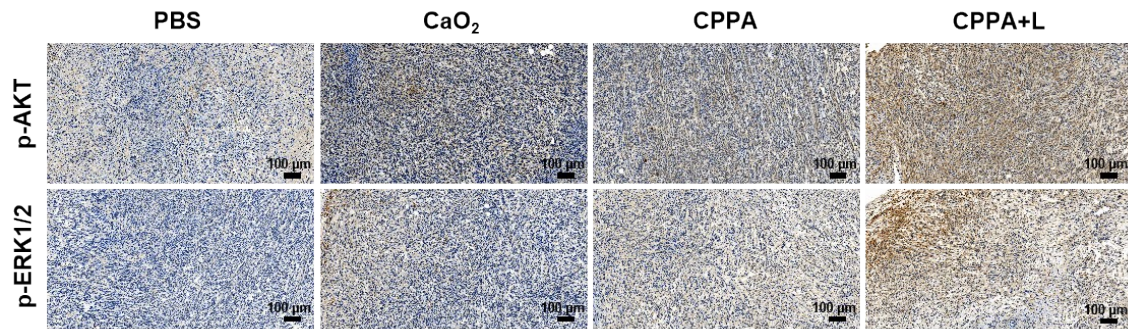


**Figure S26.** Photographs of p-AKT and p-ERK1/2 staining of tumor sections obtained from Balb/c mice subjected to different treatments. Scale bars: 100  $\mu\text{m}$ .

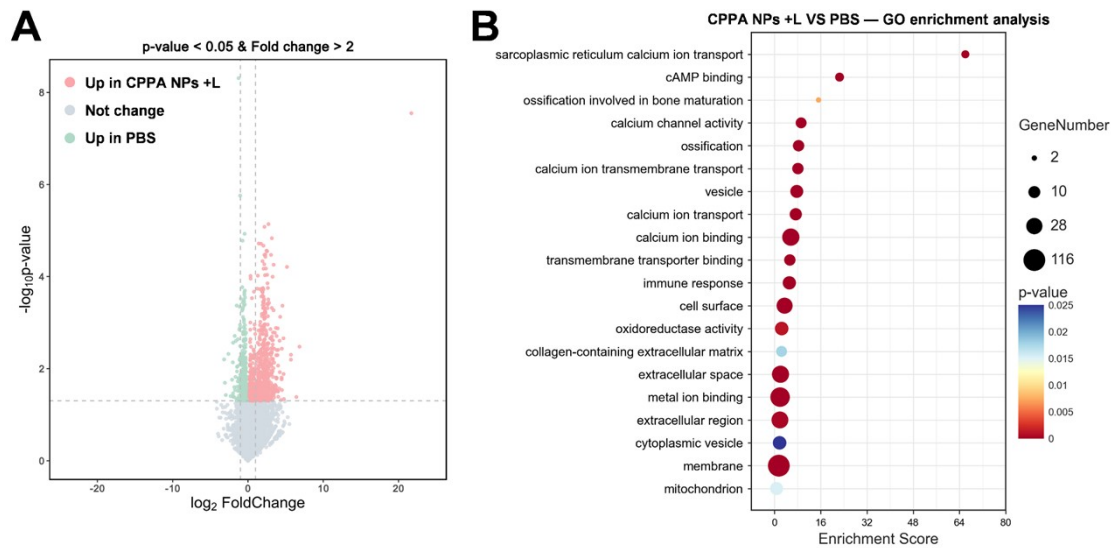


**Figure S27.** (A) Volcano plots of the up-regulated or down-regulated gene in CPPA NPs +L-PBS comparison. (B) KEGG pathway enrichment analyses were performed on differentially expressed genes (DEGs) from tumor tissues for CPPA NPs +L-PBS.